Study of the structural and spectroscopic properties of titanium oxide (TiO2 NPs): as a model of health treatment

Tamara Ail Nasser[1], Lazim Hassan aboud[2], Mohammed Abdullah Hameed[3]
[1]College of Medicine, University of Warith Al-Anbiyaa, Iraq.
[2]Department of Laser Physics, College of Science for Women, University of Babylon, Iraq.
[3]Department of Physics, College of Science/ University of Baghdad, Iraq.

Abstract
Using a DC reactant magnetron, titanium dioxide nanostructured thin films were created on glass substrates in this study. sputtering method, the plasma spraying system's operational parameters were optimized, while the sedimentation duration was varied to find the best conditions for getting high-quality samples. At various Sedimentation periods, single phase (anatase) TiO2 thin films were produced utilizing an Ar: O2 gas mixture in a 50:50 ratio (1, 1:30, 2, 2:30, 3 hours). These thin films' multilayer architectures They were made with the same mixing ratio following a one-hour sedimentation period. X-ray diffraction, atomic force microscopy, and scanning electron microscopy were used to examine the structural properties of the produced samples. The average crystal size of titanium dioxide, nitrogen, and Cu2O samples was 17.74, 22.80, and 22.81 nm, respectively, while the nanoparticles' lowest sizes were 60, 40, and 74 nm, respectively, according to the characterization data. Using an energy-dispersive X-ray spectrometer, the percentage contents of elements in the prepared samples were determined; the results revealed that the prepared samples were structurally pure. The spectral features of the samples created using UV visible light were inferred, as well as FTIR spectra, which supported the structural uniformity of the samples. The advantages of DC reactive magnetron sputtering Technique are to blame for this. Different concentrations of fluorescence and absorption spectra were tested as well.
Keywords: fluorescence, titanium oxide, uv- visible, DC reactant magnetron.

1. Introduction

Titanium dioxide nanoparticles, also known as ultrafine titanium dioxide, nanocrystal line titanium dioxide, or microcrystalline titanium dioxide, are titanium dioxide (TiO2) particles having diameters less than 100 nanometers. Because of its ability to block UV radiation while remaining transparent on the skin, ultrafine TiO2 is utilized in sunscreens. To inhibit photocatalytic processes, it has a rutile crystal structure and is covered with silica or/and alumina. The health risks of ultrafine TiO2 from dermal exposure on undamaged skin are extremely low,[1], and it is thought to be safer than other UV protection chemicals. Titanium dioxide (TiO2) has been widely reported recently for its visually appealing properties, electronic properties, and good stability in natural environments, as well as polycrystalline TiO2 films with high refractive index, wide band gap, and chemical stability for a variety of applications including optics fabrications [1], dielectric usages [2], dye sensitized solar cell (DSSC) [3], self-cleaning [4], and photocatalytic applications [5]. TiO2 can be prepared in a variety of ways, including thin films [6, 7]. Fujishima and Honda were the first to discover TiO2's photocatalytic capabilities in 1972 [8]. There are three crystalline phases of TiO2: brookite (orthorombic), anatase (tetragonal), and Rutile (tetragonal). At high temperatures, only the rutile phase possesses stable thermal dynamics. At 500 nm, the refractive index of bulk anatase and rutile titanium dioxide is roughly 2.5 and 2.7, respectively [9]. Electron beam evaporation [10], DC magnetron sputtering [5], Sol-gel technique [7], RF reactive magnetron sputtering [3], and plasma assisted chemical vapor deposition [2] are some of the deposition methods for TiO2 thin films. Dipcoating was employed to prepare thin films with a drawing speed of 9 mm/s in this study. Normal microscope slide substrates were used to deposit the films. UV-Vi's spectrometer and AFM were used to create optical, morphological, and structural profiles.

2. Experimental part

A. Preparation of Thin Film Samples

To begin the deposition procedure, the targets were cleaned and dried. Before the experiments, the glass substrates on which the thin films were deposited were cleaned. [9] On the cathode, the aim was carefully maintained. The system's operational conditions were split into two categories: constant and variable. Vacuum pressure, current limiting resistance, discharge voltage, discharge current, flow velocity, deposition temperature, inter-electrode spacing, and gas mixing ratio are among the constant working conditions. [10] Variable working conditions included deposition times of 1, 1:30, 2, 2:30, and 3 hours. The optimum operating pressure as well as the optimum mixing ratio of Ar and O2 gases were determined through a series of studies. Also, the optimal inter-electrode spacing

doi.org/10.31838/hiv23.02.146 Received: 15.10.22, Revised: 12.11.22, Accepted: 14.12.22

was discovered to be between 1 and 8 cm. Based on the findings of the studies, 4cm was chosen as the optimum inter-electrode distance. The optimum discharge current was found based on the discharge plasma's stability. To improve adhesion between the deposited layer and the substrate, the cathode was cooled by running water through the cooling channel while the anode was left to heat. [11]

B. Extraction of Nano powders from prepared thin films

The structural properties of thin film materials must be studied without interference from the substrate material on which they were deposited, which is a difficult task. The most common procedure so far has been scraping the film materials away from the substrate. These minute amounts of substrate materials can be detected using precise measurements and characterisation tests such as Fourier-transform infrared (FTIR) and energy dispersive X-ray spectrometer (EDX). As a result, the structural purity of thin-film materials cannot be guaranteed, particularly when these materials are used in applications that need extremely pure materials. In nanomaterials and nanotechnology, any approach or procedure having this attribute is favored since it reduces the likelihood of existing substrate material in the retrieved material. [14] Mechanical approaches, unfortunately, cannot solve this challenge for precise structural and spectroscopic applications. Thermal treatments are clearly avoided due to the undesired increase in nanoparticle size that results. The conjunctional freezingassisted ultrasonic extraction method, which was recently developed, is a very efficient instrument for extracting nanopowders from thin-film samples without leaving any residue from the substrate materials in the end result. The operating parameters of this approach, on the other hand, can have a reasonable impact on nanoparticle size [15].

3- Results and conclusion Thickness and time of D.C sputtering for (TiO2).

This chapter looks at the effects of working gas pressure, gas mixing ratio, inter-electrode spacing, and film thickness on the structural and optical properties of synthesized samples. The results showed that as the deposition time rose, the thickness grew, as shown in the table (1).

Table (1): The thickness and the time of D.C sputtering of (TiO2)

Materials	Deposition Time (h)	Thickness(nm)
TiO2	1	106.4
	1:30	159.6
	2	190.0
	2:30	209.0
	3	212.8

Characterization of Thin Film Structures

The structural and spectral properties of the produced samples were determined in this study. X-ray diffraction (XRD) patterns, Fourier-transform infrared spectroscopy (FTIR), atomic force microscopy (AFM), scanning electron microscopy (SEM), Energy-Dispersive X-Ray (EDX) Spectroscopy, Dispersion Curves of Nanostructured Thin Films, and UV-Visible spectroscopy are among the tests performed.

XRD Patterns of TiO_2 Films

The use of X-ray diffraction to identify the crystal structure and crystallinity is critical. Strong diffraction peaks were observed in the XRD patterns for TiO2 nanoparticles of various sizes, showing TiO2 in the anisate phase generated at a gas mixing ratio of 50:50 and a chamber temperature of 400°C. The diffraction peaks at 25.2°, 37.8°, 48.1°, 53.9°, 55.1°, 62.8°, 68.9°, 70.1°, and 75° corresponded to crystal planes (101), (004), (200), (105), (211), (118), (116), (220), and (125), which are in agreement with the standard spectrum [71], as shown in figure (3-1). Debye-equation [13] Scherer's was used to estimate the average crystallite size of the composite:

$$D = \frac{0.89\lambda}{\beta \cos\theta} \quad (4\text{-}1)$$

D is the crystallite size, 0.89 is the Scherer's constant, and 1.54056 is the X-ray wavelength. is the whole breadth at half the peak and is the Bragg angle that corresponds. The TiO2 thin film's average crystallite size was calculated to be 17.74 nanometers.

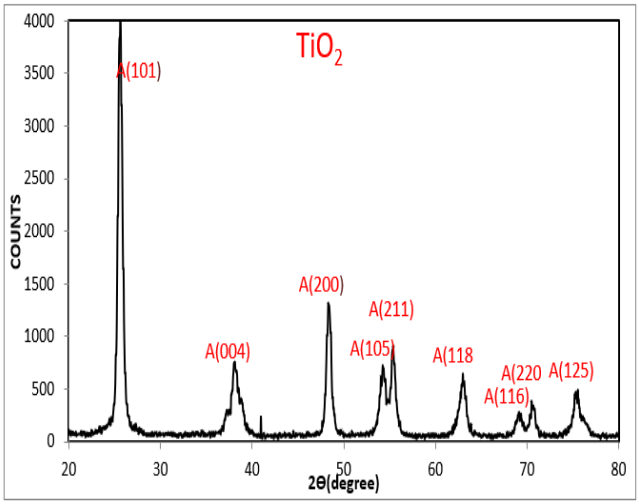

Figure (1): The XRD patterns for anatase phase of TiO_2 thin films prepared at gas mixing ratio 50:50 and inter-electrode 4 cm.

FTIR Spectra of TiO_2 Films

The use of FTIR spectra to determine the composition of metal oxides has been around for a long time. The stretching and bending vibrations of the OH group [16] cause peaks in the spectra at 3438.70 and 1640.26cm1, as indicated in the picture (3-6). For all of the produced samples, the TiO2 structure al was clearly visible in these spectra. The peak at 408.91 cm1 is attributed to Ti-O-Ti bands in the TiO2 lattice, while the band assigned to Ti-O stretching vibration was found at roughly 447 and 667 cm1. Because of the optimal working conditions utilized in the sputtering equipment, the FTIR shows that no contaminants are present inside the produced samples.

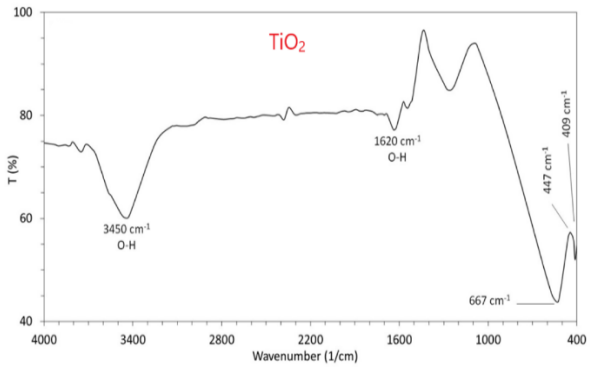

Figure (2): The FTIR spectra for TiO_2 thin films prepared at gas mixing ratio 50:50.

AFM Results of TiO_2 Films

There were various grain sizes in the TiO2 thin film. This sample had an anatase structure, which was discovered. Before reaching the substrate surface, these high-energy particles are gas-scattered as a result of collision interactions between the target and the substrate [18]. As shown in figure, the produced TiO2 nanostructures had a surface average roughness of 15.1 nm and a root-mean-squared roughness (Rr.m.s.) of 17.5 nm.

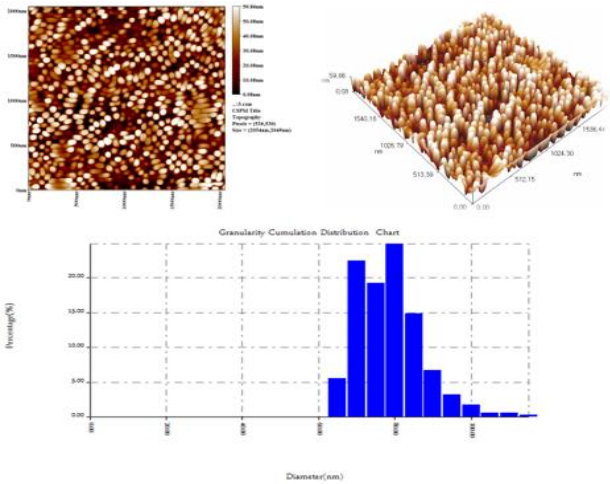

Figure (3): The three dimensional AFM micrographs and granularity cubulation distribution of TiO_2 thin film prepared at inter-electrode 4 cm and gas mixing ratio50:50 .

SEM measurements of TiO_2 Films

Scanning electron microscopy was used to determine the surface profile and particle size of the thin films produced (SEM). The homogeneity of particle distributions, which is one of the most important features of the DC magnetron sputtering process used for nanostructure fabrication, can be seen in these photos. The absence of aggregation over the scanned sample [13] is another noteworthy finding. This could be due to the TiO2 samples' heat sink mechanism, which prevents anatase from changing to rutile. This can be explained as follows: in a single phase structure, such as the anatase TiO2 sample generated in this study (see picture) (3-16). In the SEM images of nanoparticles, a hexagonal shape can be seen.

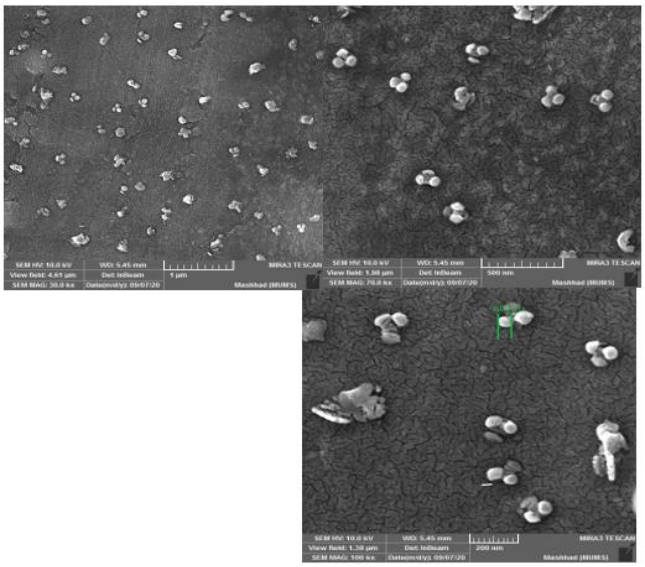

Figure (4):The SEM images of TiO_2 thin film prepared at gas mixing ratio50:50 and inter-electrode 4 cm

EDX measurements of TiO_2 Films

The produced samples' energy-dispersive x-ray (EDX) spectra were recorded and analyzed as indicated in figure (3-19). The table shows a summary of the elemental compositions in the final sample (3-2). The weight ratio of Ti:O was found to be 46.77: 50.79, based on the availability of Ti and O in the final sample. These findings supported the stoichiometry of TiO2 molecules since they matched the chemical bonding arrangement of the compound perfectly. No contaminants were found in TiO2 samples, which was corroborated by the atomic integration of Ti and O atoms. This feature is especially useful for investigations involving physical and chemical features and processes.

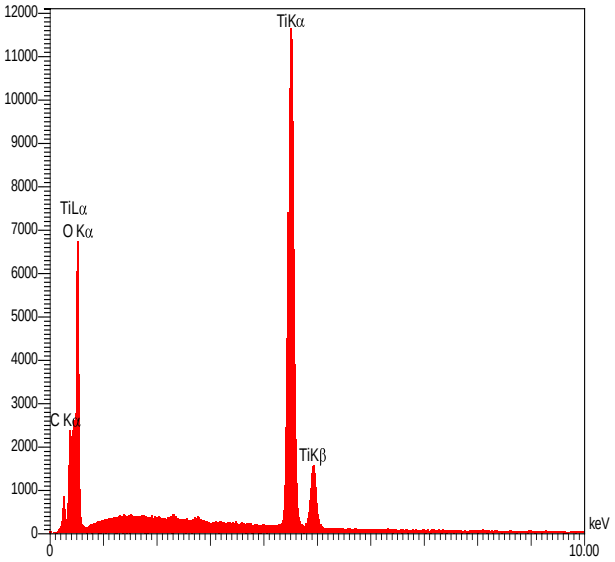

Fig.(5) :The EDX results of TiO_2 thin film prepared at gas mixing ratio 50:50 and inter- electrode 4 cm.

Table (2): Quantitative Results of TiO_2 by EDX Spectroscopy

Element	Line	Int.	W%	A%
C	Ka	80.0	2.44	4.67
O	Ka	670.5	50.79	72.91
Ti	Ka	2361.4	46.77	22.42
			100.00	100.00

4- Absorption and Fluorescence Spectra of TiO_2 NPs:

The absorption and Fluorescence spectra of the anatase phase nanocrystal line TiO_2 films in the spectral range of 200-600 nm as illustrated in Figure (6)

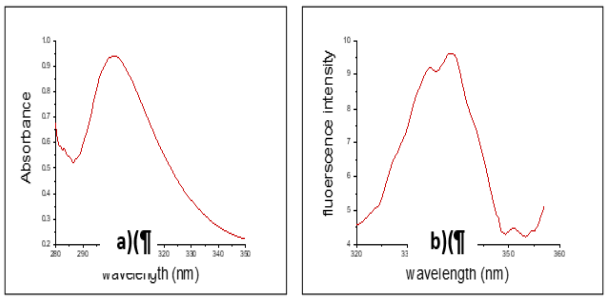

Fig. (6): a) absorption spectra for the prepared sample of TiO_2 NPs, b) Fluorescence spectra for the prepared sample of TiO_2 NPs

Figure (a) shows the adsorption spectrum of the Tio_2NPs by using uv-visible device in distilled water plotted against the wavelength (λ). The wavelength has the highest absorbance (0.941) is equal to (300 nm), since the absorption depends on the size of the particles.

Figure (b) shows the fluorescence spectrum of a Tio_2NPs using Spectra Academy device for a wide range of wavelengths (200-800) nm. The wavelength at the highest fluorescence (9.579) is equal to (340) nm. It was noticed that there is a shift towards the red wavelength compared to the absorption spectrum. The fluorescence spectrum was measured to diagnose the Tio_2NPs, as each Nanomaterial has its own fluorescence spectrum. The results are explained as in the table below:

Table (3): Results of Absorption and Fluorescence of TiO_2 NPs

Maximum peak	λmax (nm)	
0.941	301	Absorbance
9.579	340	Fluorescence

Conclusion

The following conclusions can be considered as the main outcome of this
Work:

1- The pure anatase phase structure of titanium dioxide can be prepared by careful optimization of preparation conditions and operation parameters of DC reactive magnetron sputtering technique.

2-High purity multilayer structures from titanium dioxide by same this technique.

3- titanium dioxide can be diagnosed using absorption spectra and fluorescence with high accuracy.

Reference

[1] Paolo Bettotti, "Nanodevices for Photonics and Electronics Advances and Applications," Taylor & Francis Group, LLC, 2015.dio: 10.1201/b19365.

[2] G. K. Rajan, "In-Situ Tailoring of The Morphological and Magnetic Properties of Co and CoFe Thin Film Systems," thesis, SRM University, Kattankulathur no. March 2014.

[3] Qiaobao Zhang, Kaili Zhang, Daguo Xu, Guangcheng Yang, Hui Huang, Fude Nie, Chenmin Liu, Shihe Yang , "CuO nanostructures: Synthesis, characterization, growth mechanisms, fundamental properties, and applications," Prog. Mater. Sci., vol. 60, no. 1, pp. 208–337, 2014, doi: 10.1016/j.pmatsci.2013.09.003.

[4] S. K. Ghoshal, M. R. Sahar; M.S.Rohani, and S. Sharma, , "Optoelectronics–Devices and Applications", Nanophotonics for 21 century, Textbook, 2011.

[5] A. F. Koenderink and A. Polman, "Nanophotincs: Shrinking Light-based technology," Light and Optics, May 2015. Vol. 348 ISSUE 6234. [6] F.Flory, L. Escoubas,J. Le Rouzo, and G.Berginc, " Nanophotonics," MicroNanophotonic Technol., no. February, pp.1-28, 2017, doi:10.1002/9783527699940. Ch.1.

[7] O. O. Abegunde, E. T. Akinlabi, O. P. Oladijo, S. Akinlabi, and A. U. Ude, "Overview of thin film deposition techniques," AIMS Mater. Sci., vol. 6, no. 2, pp. 174–199, 2019, doi: 10.3934/MATERSCI.2019.2.174. [8] Kiyotaka Wasa, Isaku Kanno, and Hidetoshi Kotera, "Handbook of Sputter Deposition Technology,Fundamentals and Applications for Functional Thin Films, Nanomaterials, and MEMS," Second Edition, vol.53, no.9.2013. Reference III

[9] Iyad Safi, "A study of reactive magnetron sputtering of alloy transparent conducting oxides from elemental targets", PhD thesis, Loughborough University, 1997.

[10] M. Aiempanakit, "Reactive High Power Impulse Magnetron Sputtering of Metal Oxides", Linköping Studies in Science and Technology thesis No.1519. 2013.

[11] K. O. Ukoba and F. L. Inambao, "Review of nanostructured NiO thin film deposition using the spray pyrolysis technique," Renew. Sustain. Energy Rev., no. March, pp. 0–1, 2017, doi: 10.1016/j.rser.2017.10.041. [12] S. M. Rossnagel, "Thin film deposition with physical vapor deposition and related technologies," J. Vac. Sci. Technol. A Vacuum, Surfaces, Film., vol. 21, no. 5, pp. S74–S87, 2003, doi: 10.1116/1.1600450

[13] E. A. Abdullah, "Synthesis and Spectroscopic Study of Doped TiO2 Nanostructures Using Sputtering System for Photocatalytic Applications," Thesis Submitted to the Council of College of Science, University of Baghdad ,2019.

[14] W. M. Haynes, David R. Lide, Thomas J. Bruno, "CRC Handbook of Chemistry and Physics 95thEdition," p.2666,1942.

[15] O. A. Hammadi, "Production of nanopowders from physical vapor deposited films on nonmetallic substrates by conjunctional freezing-assisted ultrasonic extraction method," Proc. Inst. Mech. Eng. Part N J. Nanomater. Nanoeng. Nanosyst., vol. 232, no. 4, pp. 135–140, 2018, doi:

10.1177/2397791418807347.
[16] A. B. D. Nandiyanto, R. Oktiani, and R. Ragadhita, "How to read and interpret ftir spectroscope of organic material," Indones. J. Sci. Technol., vol. 4, no. 1, pp. 97–118, 2019, doi: 10.17509/ijost. v4i1.15806.
[17] F. J. Al-Maliki, O. A. Hammadi, and E. A. Al-Oubidy, "Optimization of rutile/anatase ratio in titanium dioxide nanostructures prepared by DC magnetron sputtering technique," Iraqi J. Sci., vol. 60, pp. 91–98, 2019, doi: 10.24996/ijs.2019.60. S.I.14.
[18] P. Pansila and S. Chaiyakun, "Influence of sputtering power on structure and photocatalyst properties of DC magnetron sputtered TiO2 thin film Influence of sputtering power on structure and photocatalyst properties of DC magnetron sputtered TiO 2 thin film," Procedia Eng., vol. 32, no. December, pp. 862–867, 2012, doi: 10.1016/j.proeng.2012.02.024.
[19] V. Vetrivel, K. Rajendran, and V. Kalaiselvi, "Synthesis and characterization of pure titanium dioxide nanoparticles by sol- gel method," Int. J. ChemTech Res., vol. 7, no. 3, pp. 1090–1097, 2015.